Mechanics & Industry **19**, 108 (2018)
© AFM, EDP Sciences 2018
https://doi.org/10.1051/meca/2017040

Mechanics & Industry

Available online at:
www.mechanics-industry.org

Regular Article

Effect of electro-osmosis and mixed convection on nano-bio-fluid with non-spherical particles in a curved channel

N. Ijaz[1], Ahmed Zeeshan[1,*], and S.U. Rehman[2]

[1] Department of Mathematics and Statistics, FBAS, International Islamic University, Islamabad, Pakistan
[2] Department of Computer Science, University of Engineering and Technology, Taxilla, Chakwal Sub Campus, Chakwal, Pakistan

Received: 1 June 2017 / Accepted: 14 September 2017

Abstract. This paper resigns to study effects of electro-kinetic force due to presence of electrical charge layer on the walls of the channel. The nano-bio-fluid fills the void between two concentric curved plates. The flow is induced due to peristaltic wave on flexible walls. The effects of mixed convection along with heat transfer are accounted. Furthermore, the focus is on effects of shapes of non-spherical nanoparticles in nano-bio-fluid and its effects on the flow. Nanofluids are important in treatment of cancer and other diseases in tissues which are normally not reachable by normal drug procedures. The problem is modeled for four types of non-spherical nanoparticles of alumina in aqueous base fluid. Numerical solution is obtained using Mathematica. Some important results are displaced through graphs. Empirical observations display that a significantly greater velocity for nanofluid with blade shape particles is offered followed by brick shaped particles. Numerical experiment also deems a rise in heat transfer due to presence of blade shapes particles.

Keywords: Nano-bio-fluids / non-spherical nanoparticles / electro-osmosis / mixed convection / curved channel

1 Introduction

Peristaltic flows are being profusely discussed in several industrial and physiological submissions. Some of these comprise of urine transport in ureters, swallowing of food, chyme movement in the GI tract, in roller and finger pumps, etc. In all above mentioned applications, biological fluids are transported by inducing a wave on the surface of channel or tube due to contraction and relaxation of muscles along the length of tube or channel, etc. known as peristaltic wave. Study of peristaltic transport along with nanofluids and heat transfer has enriched this area a great deal. Nanotechnology has huge impact in technology world due to its extraordinary physical and chemical features. Nanofluids uses a base fluid with low thermal efficiency like water or ethylene glycol with some metallic nano-sized particles which spread uniformly throughout the fluid and consequently increase the thermal conductivity of fluid. Its applicability in phenomena like targeted drug transport, microelectronics, chiller, nuclear reactor coolant, refrigerator, fuel cells, hybrid-powered engines, space technology, pharmaceutical processes grinding and so on, brought about much interest of scientist and engineers community. Choi [1] was the first who introduced the term nanofluid. Its essential features are improvement of thermal conductivity in non-conducting or fluid with low thermal conductance. A comprehensive analysis of nanofluids was argued by Buongiorno [2]. Buongiorno argued fluids such as water (poor conductor of heat), can efficiently be used as good conductor when transformed to nanofluid, i.e. addition of metallic solids in these fluids helps to improve conductivity drastically. Many authors in recent years have taken in account the analysis of nanofluid in channel driven by peristalsis wave. Akbar et al. [3] investigate the flow of nanofluid in an asymmetric channel due to peristaltic pumping in the presence of induced magnetic field. Aly and Ebaid [4] find the exact solution for the nanofluids flowing through channel with asymmetric wave on channel wall also the slip effects are encounter for the velocity, temperature and concentration. Further, Ebaid and Aly [5] solved analytically and found exact solution for peristaltic flow in with a channel flexible wall and slip conditions. The application of the work is related to cancer treatment. The effects of hall current on flow of nanofluid through a porous channel are observed by Nowar [6]. A brief study on carbon nanofluid with heat transfer Park et al. and alumina nanoparticles, ethanol and isopropanol blend with diesel by Shaafi and Velraj [7,8]. Akram and Nadeem [9] investigate apt magnetic field on hyperbolic

* e-mail: ahmad.zeeshan@iiu.edu.pk

tangent nanofluid flowing in a channel with peristaltic transport. Akbar and Nadeem [10] show peristaltic flow of a Phan–Thien–Tanner nanofluid in a diverging tube. The flow was induced due to asymmetric peristaltic wave on the wall. Reddy and Reddy [11] study Joule heating effect due to transverse magnetic on peristaltic transport of a nanofluid in a channel with compliant walls. Akbar et al. [12] discussed interaction of nanoparticles on peristaltic flow of water base nanofluid in the presence of heat source and wall heat flux. Zamzamian et al. [13] investigated the effect of nanofluid on the efficiency of flat-plate solar collectors. Copper oxide nanoparticle made by flame spray pyrolysis for photo electrochemical water splitting e part I. CuO nanoparticle preparation. Bég and Tripathi [14] use Mathematica to simulate bio-Nano-engineering model which involves peristalsis transport along with double-diffusive convection of nanofluids. Nourani et al. [15] presented the thermal behavior of paraffin-nano-Al_2O_3 stabilized by sodium stearoyl lactylate as a stable phase change material with high thermal conductivity. They also discussed Soret and Dufour effects. Akbar [16] considered Cu-water nanofluid and saw the effects of endoscopy. Homayonifar et al. [17] devoted the Numerical simulation of Nano-carbon deposition in the thermal decomposition of methane. Nadeem et al. [18] show the flow of nanofluids in eccentric cylinders along with heat and mass transfer. Narla et al. [19] use Non-Newtonian Jeffery base fluid flowing in a curved channel. Nadeem and Maraj [20] simulate peristaltic flow of nanofluid in a curved channel with compliant walls.

The Literature mentioned shows the importance of nano bioscience in biomedical engineering, cancer treatment and targeted drugging, etc. One thing all the mentioned studies lack is the structure of nano-size particles used such as shapes and sizes. Some experimental and theoretical studies [21–25] warrant that the shape of particle tends to mark clear variation in the flow properties. Lack of such study indulges us to work and analyze this aspect of nanofluid. In this study nanoparticles of platelet, blade, cylinder and brick shapes are accounted. Mathematical equations for the flow situation and shape are modeled in a curved channel with compliant walls. The flow is induced by peristalsis wave with mixed convection and electro-osmosis effects. Using the non-dimensional parameters and assumptions of the long wavelength and low Reynolds number equations are simplified. The problem is solved numerically using 6th order RK based shooting method. The discussion of the physical phenomena is done using graphical observation.

2 Formulation of problem

2.1 Properties and shape of nanoparticles

The flow of non-spherical alumina (Al_2O_3) nanoparticles of platelet, blade, cylinder and brick shape are accounted here. It is established that all the thermal and physical quantities, i.e. density ρ_{nf}, k_{nf} is thermal conductivity of nanofluid, thermal diffusibility α_{nf}, specific heat Cp_{nf}, thermal expansion coefficient β_{nf} depends directly on concentration χ of nanoparticles and defined as

$$\rho_{nf} = \chi\rho_s + (1-\chi)\rho_f, \tag{1}$$

$$\alpha_{nf} = \frac{k_{nf}}{(\rho C_p)_{nf}}, \tag{2}$$

$$(\rho Cp)_{nf} = (1-\chi)(\rho Cp)_f + \chi(\rho Cp)_s, \tag{3}$$

$$\beta_{nf} = \frac{(1-\chi)\rho_f\beta_f + \chi\rho_s\beta_s}{\rho_{nf}}, \tag{4}$$

here the subscript f represents properties of base fluid, s defines the properties of solid nanoparticles, whereas, nf is for nanofluid.

To discuss the effects of shape of nanoparticles, the model for thermal conductivity [26], used is

$$k_{nf}/k_f = 1 + C_k^{Shape} + C_k^{Surface}, \tag{5}$$

here C_k^{Shape} and $C_k^{Surface}$ are the parameters displaying the effects of thermal conductivity due to shape of particle and resistance due to surface respectively. The shape parameter C_k^{Shape} is described by Hamilton–Crosser equation renovated by Yu and Choi [27]. The thermal conductivity model of non-spherical nano size particles are defined as [27,28] is

$$C_k^{shape} = \left(1 + \frac{m\chi X}{1-\chi_e X}\right)k_f, \tag{6}$$

X here is defined as,

$$X = \frac{1}{3}\sum_{i=a,b,c}\frac{k_{pi}-k_f}{k_{pi}-(3/\psi-1)k_f}, \tag{7}$$

here ψ is the sphericity of the particles, k_{pi} is defined as thermal conductivity along the axes of nano size particles. k_{pi} along with volume ratio and depolarization factor can be defined as [28,29]. As the nanoparticles flows through the fluid the interaction generates interfacial resistance called Kapitza resistance R_k, as interface hinders the heat flow and reduces the thermal conductivity. This gives rise to negative thermal conductivity coefficient due to surface resistance defined as,

$$C_k^{Surface} = -f\cdot l_k, \tag{8}$$

where f is the shape factor defined as normalized surface area per unit volume of the nanoparticles used and l_k is Kapitza length, defined as

$$l_k = R_k k_f. \tag{9}$$

The effective viscosity of nanofluid as defined in [27–29], due to different shapes of the particles is

$$\mu_{nf} = \mu_f(1 + A_1\chi + A_2\chi^2), \tag{10}$$

here A_1andA_2 are viscosity enhancement coefficients.

Table 1. Contribution of particles shape effect and surface resistance to thermal conductivity of nanoparticle suspensions.

Property of particles	Platelet	Blade	Cylinder	Brick
Shape	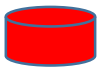			
ψ	0.52	0.36	0.62	0.81
f	2.22	3.29	0.58	0.19
l_k	1.44	1.59	1.79	1.85
A_1	37.1	14.6	13.5	1.9
A_2	612.6	123.3	904.4	471.4

Table 1 described shapes, sphericity ψ, shape factor f in 1/nm, Kapitza length l_k in nm and A_1 and A_2. The models are verified experimentally by Timofeeva et al. [30].

2.2 Electro-osmosis effects

The Poisson equation in the presence of electric Debye layer (EDL) for electric potential distribution can be written as

$$\nabla^2\tilde{\Phi} = -\frac{\tilde{\rho_e}}{\varepsilon}, \tag{11}$$

where $\tilde{\rho}_e$ is the density of the total ionic charge, ε is the permittivity, $\rho_e = e(n^+ - n^-)z$, n^+ is the number of cations and n^- is the number of anions. The Boltzmann distribution in the absence of EDL overlap, can be defined as

$$n^{\pm} = n_0 \exp\left[\pm\frac{\tilde{\Phi}ez}{k_BT}\right], \tag{12}$$

where n_0 describes the concentration of ions at bulk, which does not depend upon surface electrochemistry, e, z, k_B and T are the electron charge, charge balance, Boltzmann constant and average temperature of the electrolytic solution.

Let us define the normalized electro-osmotic potential $\tilde{\Phi}$ and zeta potential $\tilde{\zeta}$ of the medium through a medium, i.e. $\Phi' = \tilde{\Phi}/\tilde{\zeta}$

After applying the approximation of Linearized Debye-Huckel, we have

$$\sinh\frac{\tilde{\Phi}ez}{k_BT} \approx \frac{\tilde{\Phi}ez}{k_BT}. \tag{13}$$

Along with their imposed boundary conditions

$$\frac{\partial\Phi'}{\partial y}_{y=0} = 0 \text{ and } \Phi'_{y=h} = 1. \tag{14}$$

The potential can be obtained in the following form as

$$\Phi' = \frac{\cosh my}{\cosh mh}, \tag{15}$$

where m is electro-osmotic parameter which is defined as

$$m = \sqrt{\frac{2n_0}{\varepsilon k_BT}}aez = \frac{a}{\lambda_d}, \quad \lambda_d \propto \frac{1}{m}, \tag{16}$$

where λ_d is the characteristic thickness of EDL or Debye length and E is the electro-kinetic body force.

2.5 Geometry and flow problem

Alumina-water incompressible nanofluid is assumed to flow through a curved channel with semi width $\tilde{a}$. The radius of curvature is taken as $\tilde{R}^*$ with center O as displayed in Figure 1. A peristaltic wave with long wavelength λ and small amplitude $\tilde{b}$ is transmitted along the wall which induces the flow. It is assumed that the speed of wave is c and the wall is described using equation

$$H(X,t) = \tilde{a} + \tilde{b}\sin\left[\frac{2\pi}{\lambda}(X - ct)\right], \tag{17}$$

Two-dimensional velocity profile in axial and radial direction is assumed. The inertial effects are negligible. Additionally, upper and lower walls of the channel are kept at a constant temperature with lower wall at higher temperature.

The governing continuity, momentum and heat equations with effects of nanoparticles for curved channel are described as [31]

$$\frac{\partial}{\partial R}(R + \tilde{R}^*)\tilde{V} + \tilde{R}^*\frac{\partial\tilde{U}}{\partial X} = 0, \tag{18}$$

$$\begin{aligned}\rho_{nf}\left(\frac{\partial\tilde{V}}{\partial t} + \tilde{V}\frac{\partial\tilde{V}}{\partial R} + \frac{\tilde{R}^*(\tilde{U})}{(R+\tilde{R}^*)}\frac{\partial\tilde{V}}{\partial X} - \frac{(\tilde{U})^2}{(R+\tilde{R}^*)}\right)\\ = -\frac{\partial p}{\partial R}\mu_{nf}\left(\frac{1}{(R+\tilde{R}^*)}\frac{\partial}{\partial R}\left((R+\tilde{R}^*)\frac{\partial\tilde{V}}{\partial R}\right)\right.\\ + \left(\frac{\tilde{R}^*}{R+\tilde{R}^*}\right)^2\frac{\partial^2\tilde{V}}{\partial X^2} - \frac{\tilde{V}}{(R+\tilde{R}^*)^2}\\ \left. - \frac{2\tilde{R}^*}{(R+\tilde{R}^*)^2}\frac{\partial\tilde{U}}{\partial X}\right),\end{aligned} \tag{19}$$

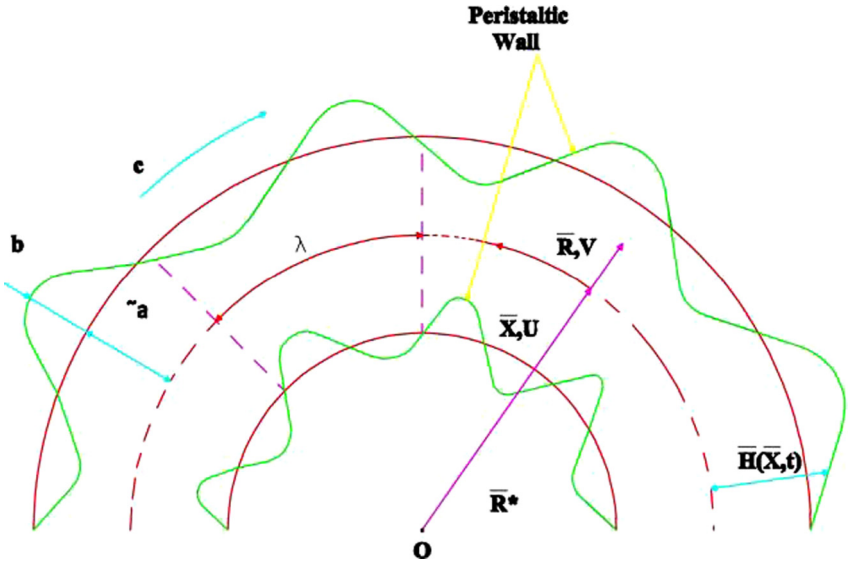

Fig. 1. Schematic diagram of the problem.

$$\rho_{nf}\left(\frac{\partial U}{\partial t}+\tilde{V}\frac{\partial U}{\partial \overline{R}}+\frac{\tilde{R}^{*}\tilde{U}}{(R+\tilde{R}^{*})}\frac{\partial \tilde{U}}{\partial X}-\frac{\tilde{U}\tilde{V}}{(R+\tilde{R}^{*})}\right)$$
$$=\frac{\tilde{R}^{*}}{(R+\tilde{R}^{*})}\frac{\partial p}{\partial X}+p_{e}E$$
$$+\mu_{nf}\left(\frac{1}{(R+\tilde{R}^{*})}\frac{\partial}{\partial R}\left((R+\tilde{R}^{*})\frac{\partial \tilde{U}}{\partial R}\right)\right.$$
$$+\left(\frac{\tilde{R}^{*}}{R+\tilde{R}^{*}}\right)^{2}\frac{\partial^{2}\tilde{U}}{\partial X^{2}}-\frac{\tilde{U}}{(R+\tilde{R}^{*})^{2}}$$
$$\left.-\frac{2\tilde{R}^{*}}{(R+\tilde{R}^{*})^{2}}\frac{\partial \tilde{V}}{\partial X}\right)+(\rho\beta)_{nf}g(T-T_{0}), \quad (20)$$

$$\left(\frac{\partial \tilde{T}}{\partial t}+\tilde{V}\frac{\partial \tilde{T}}{\partial R}+\frac{\tilde{R}^{*}\tilde{U}}{(R+\tilde{R}^{*})}\frac{\partial \tilde{T}}{\partial X}\right)$$
$$=\alpha_{nf}\left(\frac{1}{(R+\tilde{R}^{*})}\frac{\partial \tilde{T}}{\partial R}+\frac{\partial^{2}\tilde{T}}{\partial R^{2}}+\left(\frac{\tilde{R}^{*}}{R+\tilde{R}^{*}}\right)^{2}\frac{\partial^{2}\tilde{T}}{\partial X^{2}}\right)$$
$$-\frac{\mu_{nf}}{(\rho C_{p})_{nf}}\left[2\left(\frac{\partial \tilde{V}}{\partial R}\right)^{2}+\left(\frac{\tilde{R}^{*}}{R+\tilde{R}^{*}}\frac{\partial \tilde{V}}{\partial \tilde{X}}-\frac{\tilde{U}}{R+\tilde{R}^{*}}\right)\right.$$
$$\left(\frac{\partial \tilde{U}}{\partial \tilde{X}}-\frac{\tilde{U}}{R+\tilde{R}^{*}}+\frac{\tilde{R}^{*}}{R+\tilde{R}^{*}}\frac{\partial \tilde{V}}{\partial \tilde{X}}\right)$$
$$+\frac{\partial \tilde{U}}{\partial \tilde{R}}\left(\frac{\partial \tilde{U}}{\partial \tilde{R}}-\frac{\tilde{U}}{R+\tilde{R}^{*}}+\frac{\tilde{R}^{*}}{R+\tilde{R}^{*}}\frac{\partial \tilde{V}}{\partial \tilde{X}}\right)$$
$$\left.+2\left(\frac{\tilde{R}^{*}}{R+\tilde{R}^{*}}\frac{\partial \tilde{U}}{\partial \tilde{X}}+\frac{\tilde{V}}{R+\tilde{R}^{*}}\right)^{2}\right], \quad (21)$$

where $\overline{p}$ and T are fluid pressure and temperature profile, $\rho_{e}E$ is electro-osmosis term due to charged particles forming a layer on the wall of channel and $(\rho\beta)_{nf}g(T-T_{0})$ is due to mixed convection. The values for k_{nf}, α_{nf}, μ_{nf} and ρ_{nf} are obtained using equations (1)–(5) and equation (10). Last term in equation (21) represents viscous dissipation.

The problem in fixed (R, X) frame is shifted to wave (r, x) frame which is moving with the wave speed c. In wave frame velocity transformed to $(\tilde{v}, \tilde{u})$, the following translational transformations are applied

$$r=R,\ \ x=X-ct,\ \ \tilde{v}=\tilde{V},\ \ \tilde{u}=\tilde{U}-c. \quad (22)$$

Then using the non-dimensional parameters,

$$\tilde{x}=\frac{x}{\lambda},\quad r=\frac{r}{a},\quad v=\frac{v}{c},\quad u=\frac{u}{c},\quad p$$
$$=\frac{a^{2}}{\lambda\mu c}p,\quad \delta=\frac{a}{\lambda},\quad k=\frac{R^{*}}{a},\quad t$$
$$=\frac{ct}{\lambda},\quad Re=\frac{\rho ac\delta}{\mu},\quad \theta$$
$$=T-\frac{T_{1}}{T_{0}-T_{1}},\quad E=m^{2}U_{HS}\varphi,\quad Br$$
$$=\frac{\mu_{f}c^{2}}{k_{f}(T_{0}-T_{1}),}\quad Gr$$
$$=\frac{\rho_{f}g\alpha a^{2}}{\mu_{f}c}(T_{1}-T_{0}), \quad (23)$$

where Re, Gr specify the Reynolds number and Grashof number, δ, k define wave number and curvature coefficient. Using long wavelength and creeping flow assumptions equations (18)–(21) finally take the form

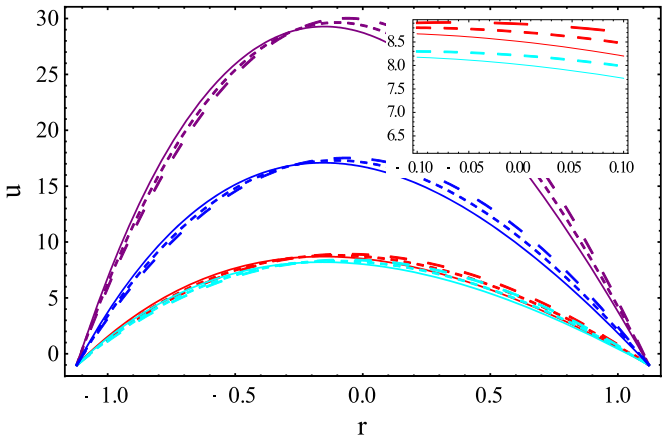

Fig. 2. Variation in velocity profile for $k=5$ (solid line),$k=10$ (dotted), $k=100$ (long dash). Purple colour indicates particle of blade shape, blue colour lines are for brick shaped particles, red lines are for platelets shaped particles and cyan colour shows behavior of cylindrical particles.

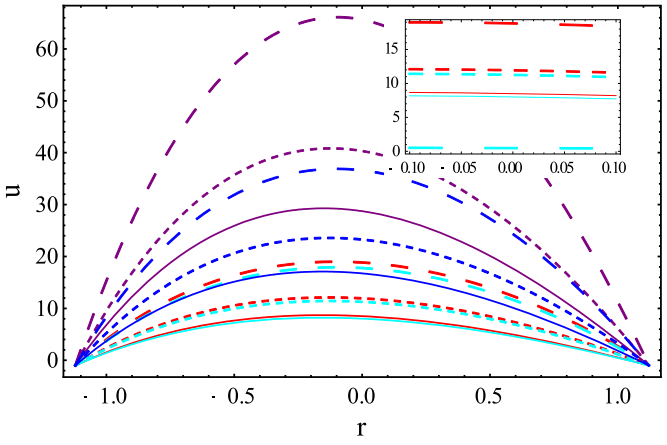

Fig. 3. Variation in velocity profile for $m=1$ (solid line),$m=3$ (dotted),$m=5$ (long dash). Purple colour indicates particle of blade shape, blue colour lines are for brick shaped particles, red lines are for platelets shaped particles and cyan colour shows behavior of cylindrical particles.

$$\frac{\mu_{nf}}{\mu(\tilde{r}+\tilde{k})^2}\frac{\partial}{\partial\tilde{r}}\left((\tilde{r}+\tilde{k})^2\frac{\partial u}{\partial\tilde{r}}\right) + \frac{\mu_{nf}}{\mu(\tilde{r}+\tilde{k})^2}\frac{\partial}{\partial\tilde{r}}\left((\tilde{r}+\tilde{k})^2\frac{u}{\tilde{r}+\tilde{k}}\right) = \frac{\tilde{k}}{\tilde{r}+\tilde{k}}\frac{\partial p}{\partial\tilde{x}} - Gr\frac{(\rho\beta)_{nf}}{\rho_f}\tilde{\theta} - m^2U_{HS}\varphi, \quad (24)$$

$$\frac{1}{(\tilde{r}+\tilde{k})^2}\left((\tilde{r}+\tilde{k})\frac{\partial\tilde{\theta}}{\partial\tilde{r}}+(\tilde{r}+\tilde{k})^2\frac{\partial^2\tilde{\theta}}{\partial\tilde{r}^2}\right) + \frac{Brk_f}{k_{nf}(1-\phi)^{2.5}}\left(\frac{\partial^2u}{\partial\tilde{r}^2}+\frac{1}{(\tilde{r}+\tilde{k})^2}(1+u)^2 + \frac{2}{(\tilde{r}+\tilde{k})^2}\frac{\partial u}{\partial\tilde{r}}(1+u)\right)=0. \quad (25)$$

We assumed the flexible walls with effects of mass per unit area, viscous damping and flexural rigidity on the plate [32–33]. The pressure gradient takes the form

$$\frac{\partial p}{\partial x} = E_1\frac{\partial^2\eta}{\partial t^2\partial x} + E_2\frac{\partial^2\eta}{\partial t\partial x} + E_3\frac{\partial^5\eta}{\partial x^5} \quad (26)$$

at $z=h(x,\ t)=1+\eta(x,\ t)$ and $\eta(x,\ t)=\varepsilon\sin2\pi(x-t)$, in which $E_1=\frac{ma^3c}{\lambda^3\mu}$, $E_2=\frac{Da^3}{\lambda^2\mu}$, $E_3=\frac{Ba^3}{c\lambda^5\mu}$.

The problem formulation completes with non-dimensional boundary conditions for velocity and temperature profile,

$$u(-h)=-1,\quad u(h)=-1,\quad \theta(-h)=1,\quad \theta(h)=0. \quad (27)$$

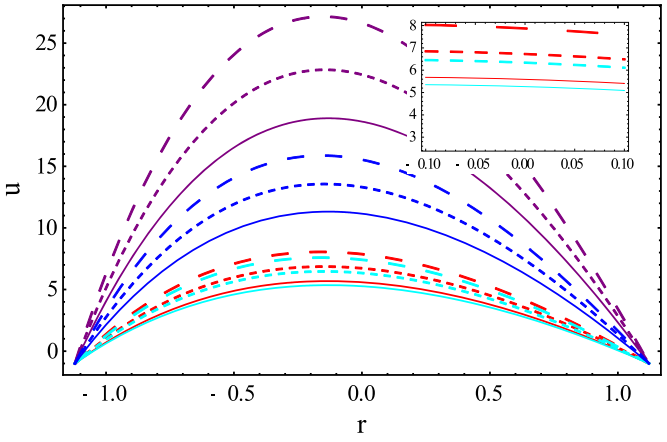

Fig. 4. Variation in velocity profile for $G_r=0.1$ (solid line), $G_r=0.3$ (dotted),$G_r=0.5$ (long dash). Purple colour indicates particle of blade shape, blue colour lines are for brick shaped particles, red lines are for platelets shaped particles and cyan colour shows behavior of cylindrical particles.

3 Graphical results and discussion

The problem is solved numerically using implicit RK with shooting scheme in Mathematica.

The variation of sundry parameters on velocity and temperature profiles is observed using graphical utility. Figures 2–4 describe the variations in velocity, while Figures 5–7 exhibit the effects of parameters on temperature profiles.

3.1 Velocity analysis

The behaviour of velocity u against r for variation in the curvature k, electro-osmostic parameter or Debye length m *and* Grashoff Number Gr. Different colours are assigned to each shape of nanoparticle to clearly distinguish between

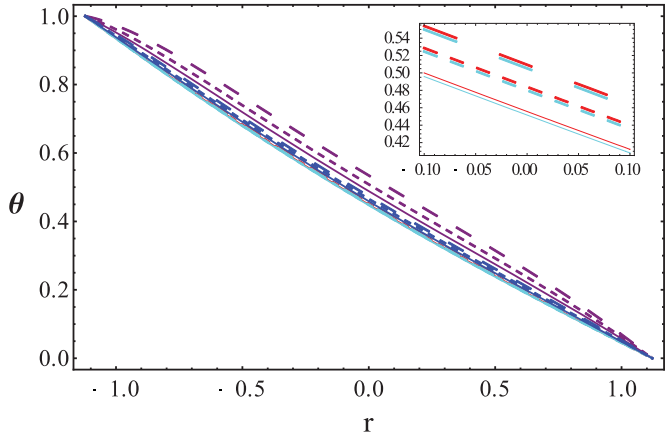

Fig. 5. Variation in temperature profile for $k=5$ (solid line), $k=10$ (dotted),$k=100$ (long dash). Purple colour indicates particle of blade shape, blue colour lines are for brick shaped particles, red lines are for platelets shaped particles and cyan colour shows behavior of cylindrical particles.

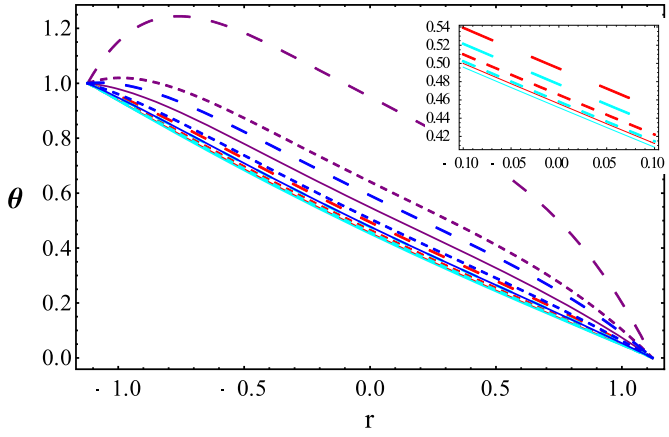

Fig. 6. Variation in temperature profile for $m=1$ (solid line), $m=3$ (dotted), $m=5$ (long dash). Purple colour indicates particle of blade shape, blue colour lines are for brick shaped particles, red lines are for platelets shaped particles and cyan colour shows behavior of cylindrical particles.

particles. Red colour indicates the platelet particles, purple colour shows the blade, cyan colour for the cylinder and blue colour fixed for the brick. Also, taking $e=0.15$, $m=1$, $U_{HS}=1$, $E_1=0.1$, $E_2=0.4$, $E_3=0.3$ are assumed as default values.

Now, the variation in velocity for different values of curvature ($k=5$, 10 100) is shown in Figure 2. It is depicted that greater curvature causes in slow down of fluid in the earlier part of the flow, i.e. the peak velocity is achieved quicker for lower curvature values. It is also observed a significantly greater velocity for nanofluid with blade shape particles as it offers minimum resistance due to flater surface, followed by brick shaped particles. Whereas, cylinder and platelets have comparable velocities, with platelets the velocity is slightly higher. Effects of electro-osmosis parameter ($m=1$, 3, 5) on velocity profile are shown in Figure 3 Influence of $m\,(1\leq m\leq 5)$ on velocity $u\,(0\leq u\leq 60)$

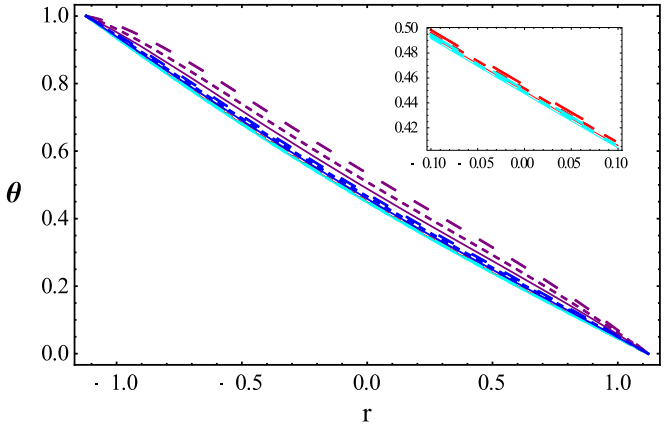

Fig. 7. Variation in temperature profile for $G_r=0.1$ (solid line), $G_r=0.3$ (dotted), $G_r=0.5$ (long dash). Purple colour indicates particle of blade shape, blue colour lines are for brick shaped particles, red lines are for platelets shaped particles and cyan colour shows behavior of cylindrical particles.

lies in greater range as compared with the previous profile of velocity $u\ (0\leq u\leq 30)$ against $k\ (5\leq k\leq 100)$, hence, flow velocity has marked an increase as m increases and the effect is consistent with all particles. It is due to the fact that value of Debye length helps by reduction of resistive force and flow is assisted by electric field generated, the results are consistent with experimental findings [34]. Also, electro-kinetic effects are similar if the effects of Helmhotz-Smoluchowski velocity U_{HS} are observed. The effects of mixed convection are observed in Figure 4 by changing Gr, between 0.1 and 0.5. It is noticed that the increase in Grashoff number increases the velocity of nanofluids.

3.2 Variations in temperature

To discuss the effects of important parameters on temperature, we have drawn Figures 5–7. Figure 5 is drawn to discuss the variation on θ for $k=5$, 10, 100. It shows that temperature increases with the increase the value of k. Also, the nanofluid with best thermal performance is with blade shape particles whereas, brick, cylinder and platelet follow, respectively. Figure 6 describes the effects of $m=1.0$, 3.0, 5.0 on θ profile. It depicts that temperature increases with the increase of the value of m. Figure 7 is drawn to discuss the effects of Grashoff number on temperature profile. The slight temperature shows the enhancement when Gr is increased.

4 Concluding remarks

This communication is a design to discuss the importance of shapes of nanoparticles in nanofluid when transporting inside a mechanical system. Four non-spherical shapes, i.e. cylinder, blade, brick and platelet shape of nanoparticles are accounted. Water-alumina nanofluid is assumed to be transported through a curved channel. The flow is induced due to peristaltic wave on the compliant wall. The effects of mixed convection and electro-osmosis due to charged particles on the wall are observed. Nanoparticle and flow

situation are modeled in form of partial differential equation with assumption of laminar and incompressible fluid along with, long wavelength of peristaltic wave on the wall. The following fallouts are concluded.

Due to low resistance of surface of blade shape particles the velocity of the fluid is maximum followed by brick, cylinder and platelet shaped particles. Again, best thermal performance is displayed by blade shape particles also, with brick, cylinder and platelet to follow respectively. These results are consistent with variation of all the displayed parameters.

The peak value of the velocity shifted to left when an increase in curvature is observed but the change is not drastic, whereas, efficiency in thermal performance is observed with greater curvature.

Velocity and temperature show a significant increase in magnitude with the increase of Debye length, i.e. electro-osmosis reduces the resistance and assists the flow.

With the increase in Grashoff number velocity and temperature increase.

References

[1] S.U.S. Choi, Enhancing thermal conductivity of fluids with nanoparticles, In: D.A. Siginer, H.P. Wang, eds., Developments and applications of Non-Newtonian flows, ASME, New York, 1995, 99–105

[2] J. Buongiorno, Convective transport in nanofluids, ASME J. Heat Transf. 128 (2006) 240–250

[3] N.S. Akbar, M. Raza, R. Ellahi, Interaction of nanoparticles for the peristaltic flow in an asymmetric channel with the induced magnetic field, Eur. Phys. J. Plus 129 (2014) 1–12

[4] E.H. Aly, A. Ebaid, Exact analytical solution for the peristaltic flow of nanofluids in an asymmetric channel with slip effect of the velocity, temperature and concentration, J. Mech. 30 (2014) 411–422

[5] A.H. Ebaid, H.E. Aly, Exact analytical solution of the peristaltic nanofluids flow in an asymmetric channel with flexible walls and slip condition: application to the cancer treatment, computational and mathematical methods in medicine, Math. Probl. Eng. (2013), doi:10.1155/2013/825376

[6] K. Nowar, Peristaltic flow of a nanofluid under the effect of hall current and porous medium, mathematical problems in engineering, Math. Probl. Eng. (2014), doi:10.1155/2014/389581

[7] S. Park, N.J. Kim, A study on the characteristics of carbon nanofluid for heat transfer enhancement of heat pipe, Renew. Energy 65 (2014) 123–129

[8] T. Shaafi, R. Velraj, Influence of alumina nanoparticles, ethanol and isopropanol blend as additive with diesel-soybean biodiesel blend fuel: combustion, engine performance and emissions, Renew. Energy 80 (2015) 655–663

[9] S. Akram, S. Nadeem, Consequence of nanofluid on peristaltic transport of a hyperbolic tangent fluid model in the occurrence of apt (tending) magnetic field, J. Magn. Magn. Mater. 358 (2014) 183–191

[10] N.S. Akbar, S. Nadeem, Endoscopic effects on peristaltic flow of a nanofluid, Commun. Theor. Phys. 56 (2011) 761

[11] M.G. Reddy, K.V. Reddy, Influence of joule heating on MHD peristaltic flow of a nanofluid with compliant walls, Proc. Eng. 127 (2015) 1002–1009

[12] N.S. Akbar, M. Raza, R. Ellahi, Influence of heat generation and heat flux on peristaltic flow with interacting nanoparticles, Eur. Phys. J. Plus 129 (2014) 185

[13] A. Zamzamian, M. KeyanpourRad, M. KianiNeyestani, M. T. Jamal-Abad, An experimental study on the effect of Cu-synthesized/EG nanofluid on the efficiency of flat-plate solar collectors, Renew. Energy 71 (2014) 658–664

[14] O.A. Bég, D. Tripathi, Mathematica simulation of peristaltic pumping with double-diffusive convection in nanofluids: a bio-Nano-engineering model, Proc. Ins. Mech. Eng. N: J. Nanoeng. Nanosyst. 225 (2011) 99–114

[15] M. Nourani, N. Hamdami, J. Keramat, A. Moheb, M. Shahedi, Thermal behavior of paraffin-Nano-Al_2O_3 stabilized by sodium stearoyl lactylate as a stable phase change material with high thermal conductivity, Renew. Energy 88 (2016) 474–482

[16] N.S. Akbar, Endoscopic effects on the Peristaltic flow of Cu-water nanofluid, J. Comput. Theor. Nanosci. 11 (2014) 1150–1155

[17] P. Homayonifar, Y. Saboohi, B. Firoozabadi. Numerical simulation of Nano-carbon deposition in the thermal decomposition of methane, Int. J. Hydrog. Energy 33 (2008) 7027–7038

[18] S. Nadeem, A. Riaz, R. Ellahi, N.S. Akbar, Effects of heat and mass transfer on peristaltic flow of a nanofluid between eccentric cylinders, Appl. Nanosci. (2013), doi:10.1007/s13204-013-0225-x

[19] V.K. Narla, K.M. Prasad, J.V. Ramanamurthy, Peristaltic transport of Jeffrey nanofluid in curved channels, Proc. Eng. 127 (2015) 869–876

[20] S. Nadeem, E.N. Maraj, The mathematical analysis for peristaltic flow of nanofluid in a curved channel with compliant walls, Appl. Nanosci. (2012), doi:10.1007/s13204-012-0165-x

[21] E. Kaloudis, E. Papanicolaou, V. Belessiotis, Numerical simulations of a parabolic trough solar collector with nanofluid using a two-phase model, Renew. Energy 97 (2016) 218–229

[22] G. Aaiza, I. Khan, S. Shafie, Energy transfer in mixed convection MHD flow of nanofluid containing different shapes of nanoparticles in a channel filled with saturated porous medium, Nanoscale Res. Lett. 10 (2015) 490

[23] F.N. Sayed, V. Polshettiwar, Facile and sustainable synthesis of shaped iron oxide nanoparticles: effect of iron precursor salts on the shapes of iron oxides, Sci. Rep. 5 (2015) 9733

[24] M.M. Bhatti, A. Zeeshan, R. Ellahi, Electromagnetohydrodynamic (EMHD) peristaltic flow of solid particles in a third-grade fluid with heat transfer, Mech. Ind. 18 (2017) 314

[25] R. Ellahi, M. Hassan, A. Zeeshan, Shape effect of nanosize particles in Cu-H_2O nanofluid on entropy generation, Int. J. Heat Mass Trans. 81 (2015) 449

[26] E.V. Timofeeva, J.L. Routbort, D. Singh, Particle shape effects on thermophysical properties of alumina nanofluids, J. Appl. Phys. 106 (2009) 014304

[27] W. Yu, S.U.S. Choi, The role of interfacial layers in the enhanced thermal conductivity of nanofluids: a renovated Hamilton-Crosser model, J. Nanoparticle Res. 6 (2004) 355–361

[28] R. Ellahi, M. Hassan, A. Zeeshan, Shape effects of spherical and nonspherical nanoparticles in mixed convection flow over a vertical stretching permeable sheet, Mech. Adv. Mater. Struct. (2016) 1232454, DOI:10.1080/15376494

[29] A. Zeeshan, M. Hassan, R. Ellahi, M. Nawaz, Shape effect of nanosize particles in unsteady mixed convection flow of nanofluid over disk with entropy generation, Proc. Inst. Mech. Eng. E: J. Process Mech. Eng. (2016) 0954408916646139
[30] E.V. Timofeeva, J.L. Routbort, D. Singh, Particle shape effects on thermophysical properties of alumina nanofluids, J. Appl. Phys. 106 (2009) 014304
[31] S. Nadeem, I. Shahzadi, Mathematical analysis for peristaltic flow of two phase nanofluid in a curved channel, Commun. Theor. Phys. 64 (2015) 547
[32] M.M. Bhatti, A. Zeeshan, R. Ellahi, N. Ijaz, Heat and mass transfer of two-phase flow with electric double layer effects induced due to peristaltic propulsion in the presence of transverse magnetic field, J. Mol. Liq. 230 (2017) 237–246
[33] S. Nadeem, A. Riaz, R. Ellahi, Peristaltic flow of a Jeffrey fluid in a rectangular duct having compliant walls, Chem. Ind. Chem. Eng. Q 19 (2013) 399–409
[34] P. Goswami, J. Chakraborty, A. Bandopadhyay, S. Chakraborty, Electrokinetically modulated peristaltic transport of power-law fluids, Microvasc. Res. 103 (2016) 41–54
[35] B.C. Liechty, B.W. Webb, R.D. Maynes, Convective heat transfer characteristics of electro-osmotically generated flow in microtubes at high wall potential, Int. J. Heat Mass Trans. 48 (2005) 2360–2371
[36] R. Ellahi, M. Hassan, A. Zeeshan, Aggregation effects on water base Al_2O_3-nanofluid over permeable wedge in mixed convection, J. Chem. Eng. 11 (2016) 197–186

Cite this article as: N. Ijaz, A. Zeeshan, S.U. Rehman, Effect of electro-osmosis and mixed convection on nano-bio-fluid with non-spherical particles in a curved channel, Mechanics & Industry **19**, 108 (2018)